

Introducing a Novel Analysis Technique for Osseointegrated Dental Implants Retrieved 29 Years Postsurgery

Hamid Sarve, MSc PhD-student;* Bertil Friberg, DDS, MDS, PhD;† Gunilla Borgefors, MSc, PhD;‡ Carina B. Johansson, PhD§

ABSTRACT

Purpose: To investigate osseointegration of oral implants, which were retrieved from a patient after 29 years in situ, we use novel three-dimensional analysis methods and visualization techniques that supplement conventional two-dimensional analysis.

Materials and Methods: The sample processing involved nondecalcification and embedment in resin. Conventional two-dimensional histomorphometrical methods were conducted. Additionally, the quantification was extended to three-dimensional by using synchrotron radiation micro-computed tomography (SR μ CT) technique and two relevant visualization methods for the three-dimensional data were introduced.

Results: The three-dimensional results involved three-dimensional quantification and visualization of two implant samples with methods beyond state-of-the-art. Traditional two-dimensional histomorphometrical results revealed a mean bone-implant contact (BIC) of about 50%. In most samples, bone area (BA) was lower inside the treads compared with out-folded mirror images, which were confirmed by the three-dimensional quantification. The BIC along four selected regions showed highest percentages in the bottom/valley region and lowest in the thread-peak region. Qualitative observations revealed ongoing bone remodeling areas in all samples. The apical hole demonstrated high osseointegration.

Conclusion: The novel techniques including an animation and an out-folding of BIC and BA enabled a simultaneous visualization of the three-dimensional material obtained from SR μ CT data. However, the two-dimensional histological sections were needed for qualitative and quantitative evaluation of osseointegration and, thus, both methods are considered equally important.

KEY WORDS: animation, case report, osseointegration, SR μ CT, undecalcified cut and ground sections, visualization

INTRODUCTION

Retrieval of oral implants with subsequent histological and sometimes quantitative histomorphometrical analyses that result in case reports, is rather frequently reported in the literature and most of which involve

investigations using cut and ground sections.¹⁻⁴ These case reports are of value for documentation of scientific observations at the time of retrieval and might serve as historical documents. Therefore, it is important to document and report what we observe in specific cases, albeit today we may not fully understand the reasons behind tissue reaction.

Case report studies of retrieved human implants including investigation of osseointegration with computed tomography methods are sparse. In a paper by Rebaudi and colleagues,⁵ a microimplant was retrieved from a patient 12 months after insertion. The authors report bone-implant apposition in a region of 45 μ m from the implant.⁵ Retrieval of implants from animal studies involving micro-computed tomography (μ CT) are more and more frequently found in the literature.^{6,7}

*PhD student, Centre for Image Analysis, Swedish University of Agricultural Sciences, Uppsala, Sweden; †associate professor, Brånemark Clinic, Göteborg, Sweden; ‡professor, Centre for Image Analysis, Swedish University of Agricultural Sciences, Uppsala, Sweden; §professor, Institute of Odontology, Department of Prosthodontics/Dental Materials Science, University of Gothenburg, Göteborg, Sweden

Reprint requests: Mr. Hamid Sarve, Centre for Image Analysis, Swedish University of Agricultural Sciences, SE-75 105 Uppsala, Sweden; e-mail: hamid@cb.uu.se

© 2011 Wiley Periodicals, Inc.

DOI 10.1111/j.1708-8208.2011.00413.x

None of the three mentioned studies reported “direct” bone-implant contact (BIC) data. A recently published paper suggested a new method of evaluating osseointegration, that is, bone contact area as a measure of osseointegration within a distance of 35 μm from the implant surface.⁸ Comparisons of traditional μCT to synchrotron radiation μCT (SR μCT) have been reported in a few studies.⁹ Yet another comparison of results obtained using SR μCT and μCT revealed the former to produce less blurry images compared with μCT .¹⁰ The authors of the present paper point out the difficulties in capturing various gray levels in bone. This latter methodological issue is, however, not included in the present study.

The current paper aimed at investigating and describing a set of five retrieved original Brånemark implants from one patient being treated with oral implants in 1978. The implants had been in situ for 29 years prior to retrieval. Both state-of-the-art and conventional histological and histomorphometrical analyses were included. Moreover, selected samples were utilized in a three-dimensional analysis, with an animation that allows the observer to follow the osseointegration in a simultaneous three-dimensional “thread-fly-through” slide, as well as a novel “two-dimensional unfolding,” which mapped the implant surface, with projected feature information, to a two-dimensional image.

MATERIALS AND METHODS

Patient History

This case report involves a female patient born in 1943 with edentulous maxilla since 1964. The patient received

six implants (original Brånemark fixtures with a length of 10 mm in the spring of 1978). The patient had abutment connection in February 1979 and was equipped with a fixed prosthesis 1 month later. At the time of implant insertion, the patient was healthy and has no intake of medicines. The patient was a heavy smoker, although no data are available on the daily cigarette consumption.

At abutment connection, the patient presented 2–4 mm of marginal bone loss mainly at the fixtures on the left-hand side, albeit at the 1-year follow-up (March 1980) all implants showed the same pattern of crater-shaped marginal bone resorption (Figure 1). During the years until the 10-year follow-up visit (Figure 2), radiographic examinations revealed stabilized marginal bone levels with only minor alterations and according to the examining dentists, the patient maintained an optimal oral hygiene. However, the mandibular dentition was afflicted with periodontal disease, which is allegedly regarded one major risk factor for the development of peri-implantitis.¹¹ At the 15-year follow-up, progression of bone loss around #L3 (left posterior implant) was seen with bleeding and pus on probing. Explorative surgery revealed a fracture of the implant #L3, which was thus repaired to continuously support a remade fixed prosthesis (Figure 3).

Several annual checkups were executed between years 15 to 27 of follow-up, occasionally showing some implants with clinical symptoms of mucositis, although with rather stable radiographic bone levels. In 2005, the titanium prosthetic framework fractured close to the midline and a fracture of implant #R3 (right posterior implant) was discovered, which could not be repaired

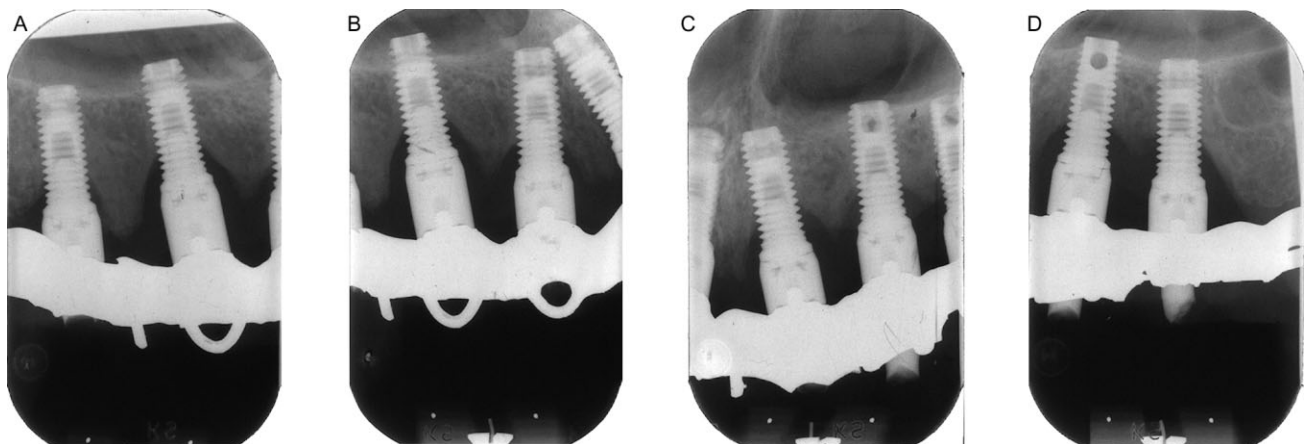


Figure 1 Similar radiographic bone resorption pattern around all six implants at the 1-year checkup. The figures represent: (A) R3, R2; (B) R2, R1; (C) L1, L2; (D) L2, L3.

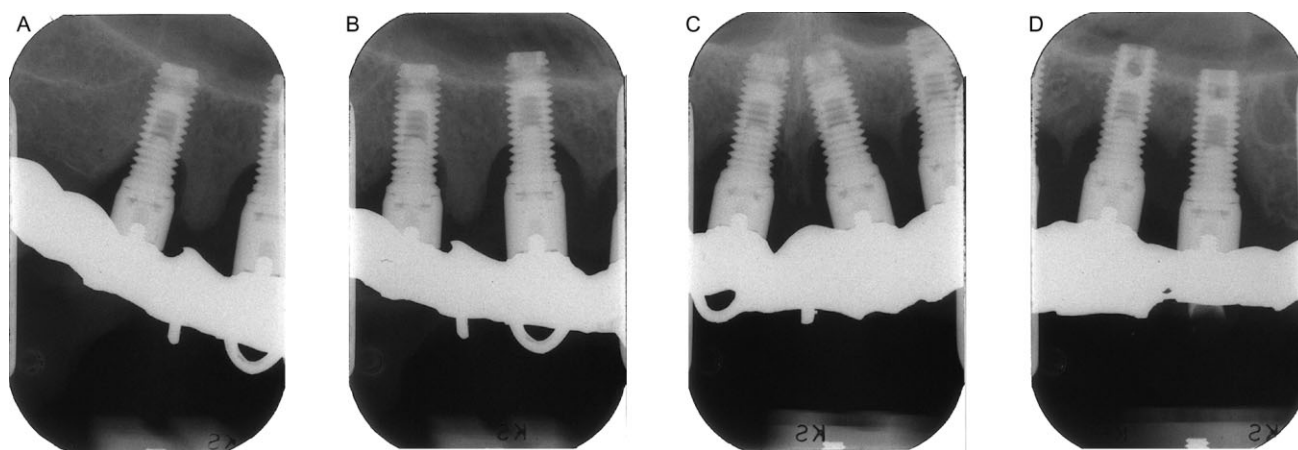


Figure 2 Marginal bone levels at the 10-year follow-up visit. Some further bone resorption has occurred, as compared with the 1-year checkup. The figures represent: (A) R3; (B) R3, R2; (C) R1, L1; (D) L2, L3.

(Figure 4). The fixed prosthesis was reduced to a total of eight teeth. Implant #L3 was found mobile and removed in 2006. This sample is not included in the present report.

Clinical soft-tissue problems and mechanical complications due to overload were constantly present from now on and in 2007 (29 years after implant placement). It was decided to trephine out all remaining implants including fractured fragments in order to preserve the maxillary bone for later implant reoperation. After testing a removable complete denture, the patient was not motivated to undergo further surgery, though.

Sample Preparation

The five implant samples, retrieved with a trephine drill, were immersed in 4% neutral-buffered formaldehyde, dehydrated in ethanol (70–99%), preinfiltrated in diluted resin and infiltrated in pure resin, followed by embedding in pure resin (in cylinders with a diameter of 1.5 cm) and

curing under ultraviolet light (Technovit 7200 VLC, Kulzer, Germany), according to the internal laboratory guidelines at the Department of Biomaterials, Gothenburg university, Göteborg, Sweden. The resin-embedded, nonfractured samples ($n = 2$) were selected for three-dimensional analysis (see later section) before sectioning. The Exakt equipments (Exakt Apparatebau, Norderstedt, Germany) were used for preparation of undecalcified cut and ground sections with the implant in situ.^{12,13} After three-dimensional SRμCT imaging, the five resin-embedded samples were divided in longitudinal manner of the implant. One central section of 15 μm was prepared from each sample. Sections were stained in toluidine blue mixed with pyronin G, rinsed in water, dried in air and cover-slipped prior to qualitative and quantitative evaluation in the light microscope. The latter involved computer-based analysis (using the Leitz Aristoplan light microscope coupled to a Microvid unit and a PC enabling analysis to be performed directly in the eyepiece of the

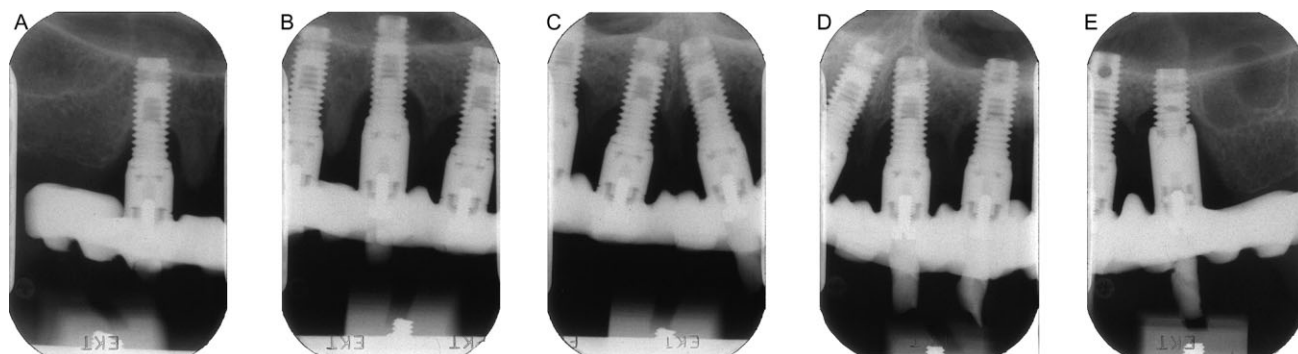


Figure 3 Fracture of implant #L3 (E), which was repaired for further function. The figures represent: (A) R3; (B) R2, R1; (C) R1, L1; (D) L1, L2; (E) L3.

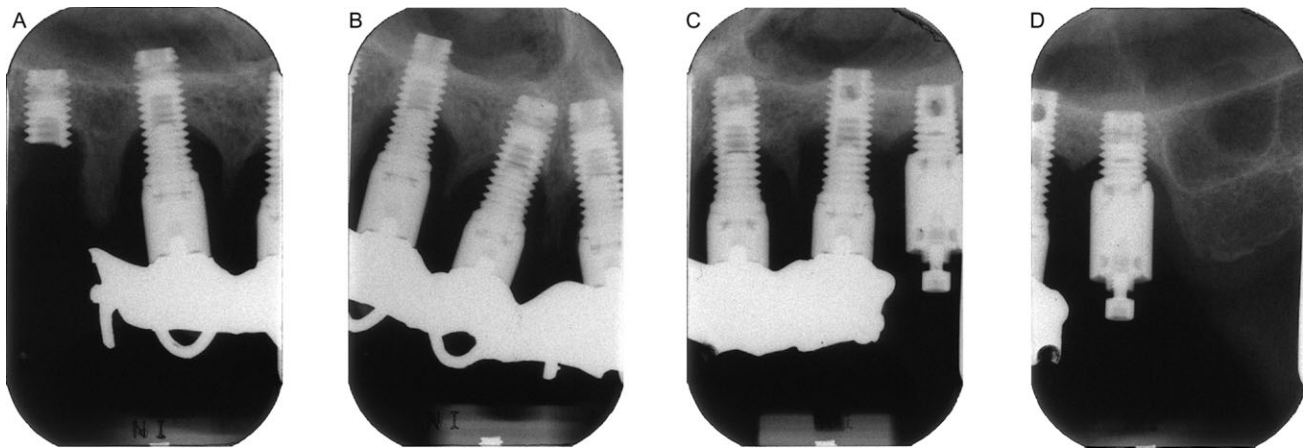


Figure 4 Condition of implants after 26 years. Fractured implant #R3 could not be repaired. The figures represent: (A) R3, R2; (B) R2, R1; (C) L1, L2; (D) L3.

microscope) of BIC, bone area (BA) inside the threads, and in the out-folded mirror images (MI) to the inner threads.¹⁴ Moreover, bony contacts were measured along a selected portion of the implant surface revealing BIC at four different locations along an implant thread, that is, the bottom portion of the implant, the upper flank portion, the tip of the implant, and the lower flank region.⁴ This division of BIC illustrated in selected portions is most likely related to the bone-remodeling pattern (BRP) and elaborated on in the paper by Bolind and colleagues.⁴ This way of presenting osseointegration is, according to the authors, a new approach and may render an increased knowledge related not only to the BRP around the threads but also it may add knowledge related to bone loading conditions.

Computed Tomography

Implant samples are commonly imaged using standard μ CT devices. However, a number of artifacts are associ-

ated with μ CT,¹⁵ and some of them occur particularly when the samples include metal particles, such as titanium implants. Dense objects absorb a considerably higher amount of x-rays than less dense objects.^{9,16} This leads to artifacts, such as an edge gradient, which surrounds the implant and hides substantial information close to the implant interface. This artifact prevents reliable discrimination between the bone and soft tissue close to the implant, which is actually the most important region to analyze.

Nevertheless, the impact of artifacts can be reduced largely by using another μ CT technique, that is, the SR μ CT. This technique yields more accurate tomographic reconstructions, has a higher signal-to-noise ratio, and avoids the beam-hardening artifacts¹⁷ due to parallel beam acquisition and monochromatic beams. The edge gradient effect, described previously, is smaller in SR μ CT-acquired images, even though the artifact cannot be removed entirely.

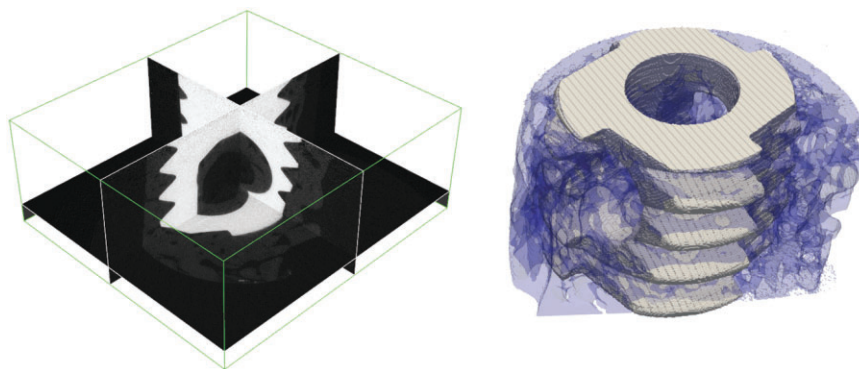


Figure 5 (Left) Three-dimensional volume of implant sample A. (Right) Rendering of the segmented volume. The white region represents the implant and the blue region represents the bone tissue. The opacity of the bone tissue region is decreased to enable visualization of the cavities.

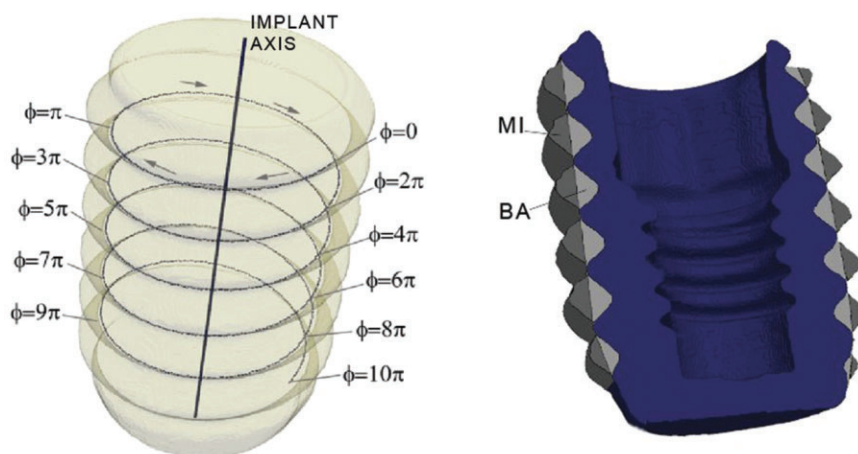


Figure 6 (Right) Different positions along the helix of the implant and corresponding Φ -values for an implant with five threads. (Left) Features in the region of interest. The implants shown here have been inserted in rats and are not part of this case study.

The two selected nonfractured implant samples were scheduled for SR μ CT at the facility GKSS (Gesellschaft für Kernenergieverwertung in Schiffbau und Schifffahrt mbH) at HASYLAB (Hamburger Synchrotronstrahlungslabor), DESY (Deutsches Elektronen-Synchrotron) in Hamburg, Germany.

The imaged volumes were segmented into regions of bone tissue, soft tissue, and implant using the method described in Sarve and colleagues¹⁶ (Figure 5). The implant is a low-noise region with homogenous intensity in the image volume and is easily segmented using thresholding. The bone and soft tissue, on the other hand, are more difficult to distinguish as they have intensity values close to each other, especially in the regions close to the implant. As mentioned, the volume suffered from edge gradient artifacts close to the implant boundary (although reduced as SR μ CT technique was used), which appeared as a graded transition from high intensity to low. A correction method¹⁶ was applied prior to the segmentation to compensate for the artifact to avoid misclassification of the affected voxels.

After the artifact correction, linear discriminant analysis (a supervised classification method) is used to segment bone and soft tissue. This method requires a training step, that is, sample regions of the bone and soft tissues are marked manually in one slice of the volume.

Instead of only preparing “interesting illustrations,” which are included in most papers related to retrieved implants with further CT applications, our aim was to actually perform quantifications of bone tissue surrounding the implants that possibly can be referred to as osseointegration. With this in mind, we extended

the traditional two-dimensional features to three-dimensional. The implant was modeled as a helix followed by quantification of the features for all angles: $BIC(\phi)$, $BA(\phi)$ and $MI(\phi)$, where $\phi \in [0, 2\pi t]$ denotes the rotation about the implant axis and t is the number of thread turns (Figure 6). The features, and the method for the extraction of them, were introduced in Sarve and colleagues.¹⁸ Extraction of these features from the volume provides lower precision compared with histological sections. But on the other hand, this method gives an overview of the whole distribution of the bone around the observed implant. To the best of our knowledge, this visualization method related to osseointegration of clinical implants has not been presented before.

In addition to the three-dimensional feature extraction, two visualization methods are used to enable easy highlighting of relevant information. The first one, similar to the above-mentioned three-dimensional feature extraction, “thread-fly-through,”¹⁹ follows the helix-shaped implant thread from the top of the implant to the bottom and extract $n = 2,880$ local slices from the image volume, which are assembled into an animation. Along with the slices, traditional features revealing information about the bone-implant integration are computed and presented. The features involve bone ratio in the region around the thread peak (BA) and BIC for the same region.

The second method, “two-dimensional unfolding,”¹⁹ renders a cylindrical unfolding of the implant surface on which feature information has been projected to a two-dimensional image. The relevant feature information (BA or BIC) is projected onto the implant

surface and each slice of the surface is unfolded to a row in the two-dimensional image by an angular sampling. The sampling is made from the implant axis as origin.

RESULTS

Implant threads are often damaged when the implant and its surrounding bone is retrieved using a trephine drill. This was the case also with the present sample retrieval. However, at least 50% of the implant geometry was preserved rendering adequate information as well as material (i.e., bone tissue surrounding implant) for subsequent preparation to cut and ground sections.

SR μ CT

The resin-embedded cylindrically shaped samples required a scanning time of 4 hours each. Two implant samples were imaged.

Altogether 1,440 equally stepped radiograms were acquired between 0° and 360°. A filtered-back projection algorithm was used to obtain the three-dimensional data of x-ray attenuation for the samples. The field of view of the x-ray detector was set to 6.76 × 4.51 mm with a pixel size of 4.40 μ m, providing a reconstructed image volume of 14.3 × 14.3 × 5.5 mm with a measured spatial resolution of about 11 × 11 × 11 μ m.

The extraction of features in three-dimensional resulted in six graphs, shown in Figure 7, illustrating the respective feature for each angle, ϕ , when traveling along the implant helix of the two implants. The respective graphs have been smoothed by a Gaussian low-pass filter with a standard deviation of 0.2 to improve visualization of the plots. Moreover, the mean values of the different features, which are averaged over the complete helix, are shown in Table 1.

The three-dimensional data were visualized by an animation (see attached media, a snapshot is also shown

in Figure 8) related to what the present authors determine as the “thread-fly-through.” Using this modality, the observer can get visualized information about the osseointegration of all angles. The animations, however, are speeded up in order to reduce the file size, resulting in 350 slices per turn.

Yet another way of presenting the three-dimensional data in a two-dimensional manner resulted in the concept named “two-dimensional unfolding,” thus, being another way of presenting an immediate overview of the feature information. Figures 9 and 10 demonstrate, a fast overall perception of the features with no rotation or any other transformation of the volume needed is shown to the observer. Irrespective of three-dimensional animation “thread-fly-through” or “two-dimensional unfolding,” both techniques are, according to the authors, novel approaches for researchers in the biomaterials field evaluating osseointegration.

Light Microscopy Analysis

Histomorphometry. In general, there were no major quantitative differences between the nonfractured and fractured samples. The mean value of BIC for the two intact implants (involved in SR μ CT) was a bit lower (49%) compared with the three fractured implants (52%) (Figure 11).

Both BA and MI were higher for the two intact samples (mean value 70% and 78%, respectively) and lower for the three fractured mean value (65% and 61%, respectively) (Figure 11). Taken the five implants together the mean numbers were for BIC 50%, BA 78%, and MI 78% as well.

The BRP in the four different regions along the thread profile revealed some differences when comparing individual portions. In general, the thread-peak region demonstrated the lowest BIC (27%) while the bottom part, on the other hand, had the greatest BIC (58%). Despite the limited number of samples ($n = 5$) and unknown actual loading time, the lowest BIC was observed in the thread-peak region while the highest BIC was observed in the bottom region. Observations on the two intact implants demonstrated the greatest BIC in the bottom portion and the lowest BIC percentages in the lower flank region. The greatest BIC of the three fractured implants was the bottom region, and the lowest BIC in the thread-peak region (Figure 12). Comparison of the mean values from all four portions with the traditional BIC measurements demonstrated a

TABLE 1 Mean Value for Bone-Implant Contact (BIC), Bone Area (BA) inside the Threads, and in the Out-Folded Mirror Images (MI). The Data Have Been Sampled along the Helix-Shaped Implant Thread and Averaged over the Complete Thread

	Mean Value BIC	Mean Value BA	Mean Value MI
Implant 239	54.9%	53.8%	45.0%
Implant 240	69.1%	34.9%	55.5%

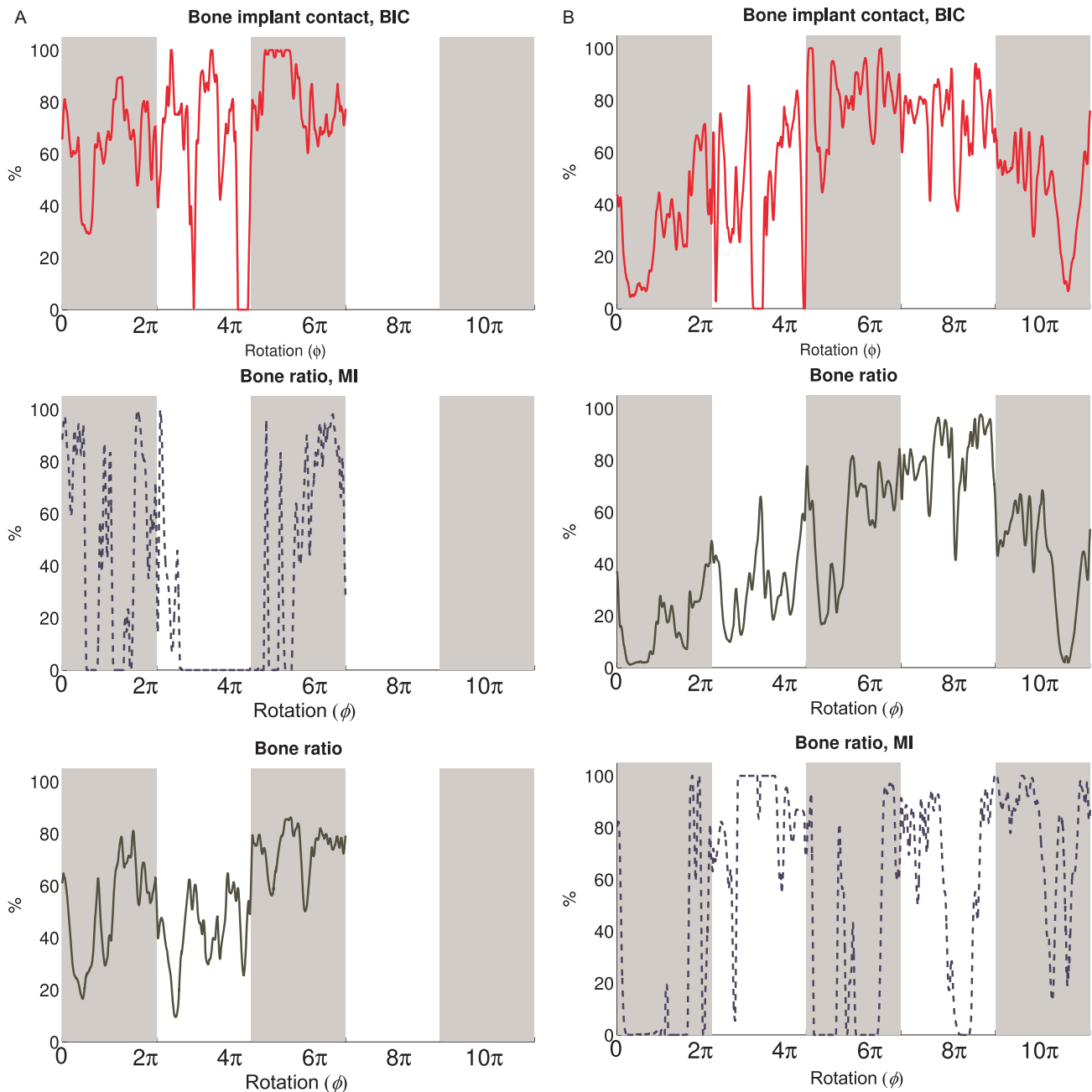


Figure 7 (A) Quantified features; BIC (Φ) (top), BA (Φ) (middle), and MI (Φ) (bottom) for implant 239. The features are shown along the implant threads with respect to rotation angle Φ . The implant has been partially damaged during the extraction process. Therefore, it has not been possible to evaluate all threads. (B) Quantified features; BIC (Φ) (top), BA (Φ) (middle), and MI (Φ) (bottom) for implant 240. The features are shown along the implant threads with respect to rotation angle Φ . Each marked region (with altering background color) indicates one thread.

mean difference of 19% larger numbers for the latter technique, which does not take the thread peaks in consideration.

Qualitative Observations

In general, the survey pictures of samples demonstrated the upper half of the implants to be absent of tissue,

thus, about 50% of the implants were nonosseointegrated. The two nonfractured implants were engaged with bone tissue in eight threads, compared with six threads in the three fractured samples.

The qualitative observations of the tissue structures surrounding the implant revealed a more spongy type of bone surrounding the fractured implants while

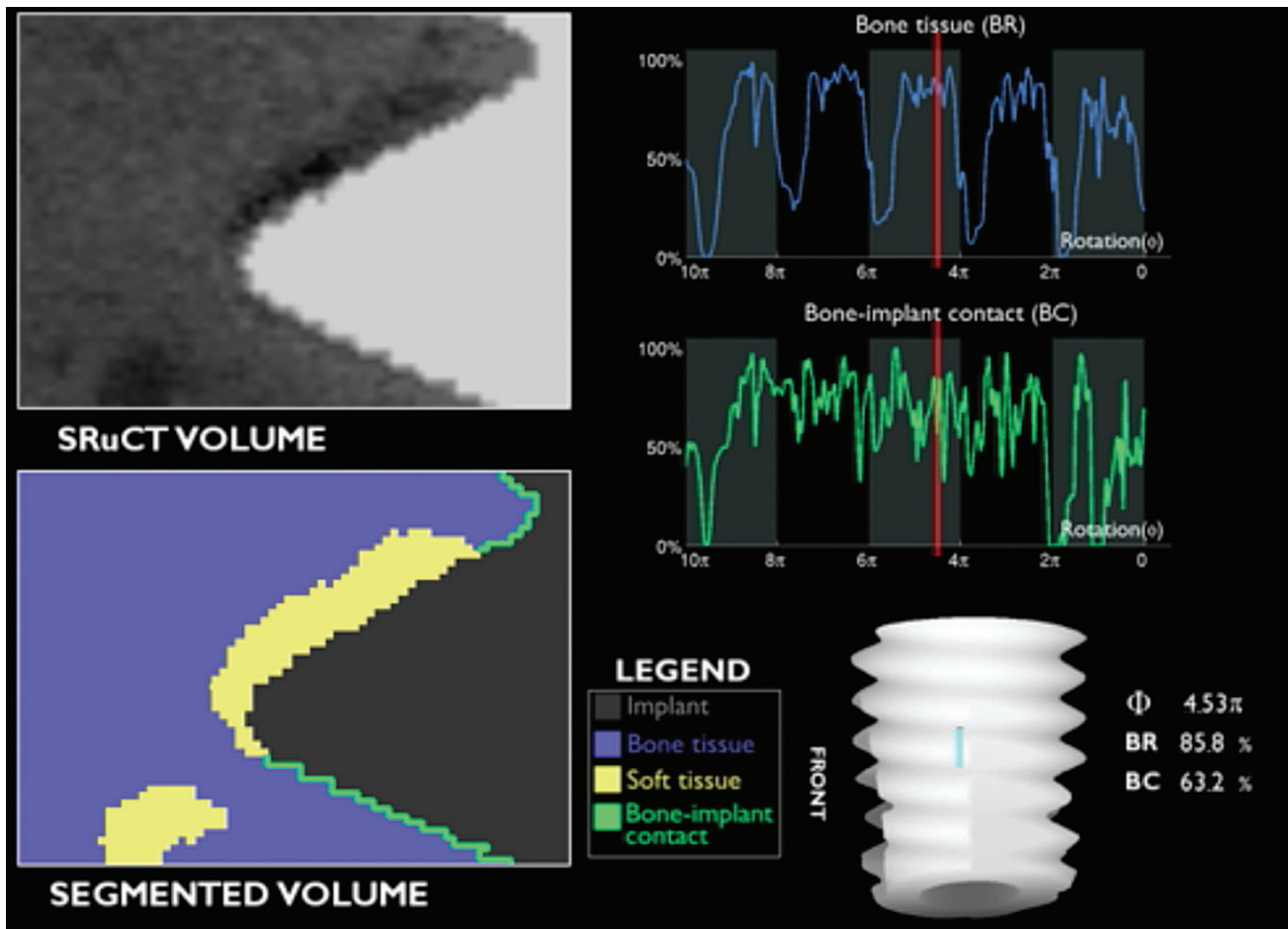


Figure 8 Snapshot of one thread-fly-through animation (of implant 240).

the two intact screws had a more compact/cortical bone appearance. Cement lines were clearly visible structures in the bone and mostly mature osteocytes were seen but some regions with darker stained bone tissue and large osteocytes were observed, indicative of less mature bone tissue/bone forming regions. Bone remodeling cavities could be observed and in some areas, osteoid, together with osteoblast, was observed in close relation to the implant surface. The apical hole revealed a quite extensive amount of bone tissue with a high degree of BIC (Figure 13, A and B). In higher magnification, soft-tissue regions with inflammatory cells could be seen.

DISCUSSION

The present case report describes the fate of five (six) titanium implants (Brånemark System®, Nobel Biocare, Zürich, Switzerland), supporting a fixed construction in the maxilla, for a period of up to 29 years. The somewhat increased marginal bone loss experienced at abutment

connection and during the first year of function may to a great extent be explained by the bone-remodeling process initiated to withstand load forces from the implants. Irrespective of intact or fractured samples, the BIC was similar, that is, 49% and 52%, respectively. The three fractured implants demonstrated lower BA and MI (65% and 61%, respectively) compared with the two intact implants (70% and 78%, respectively), which most likely can be explained as a result of stress in the region of interest and perhaps this stress may have induced greater bone resorption around the fractured fragments. However, the heavy smoking behavior of the patient may also have influenced tissue quality and quantity and therefore contributed to the bone loss. The marginal bone levels were quite stable for the subsequent 14 years and, thus, the initial bone loss was not accompanied by a continuous loss during that period. This is an important piece of information, because marginal bone resorption to such an extent, may frequently

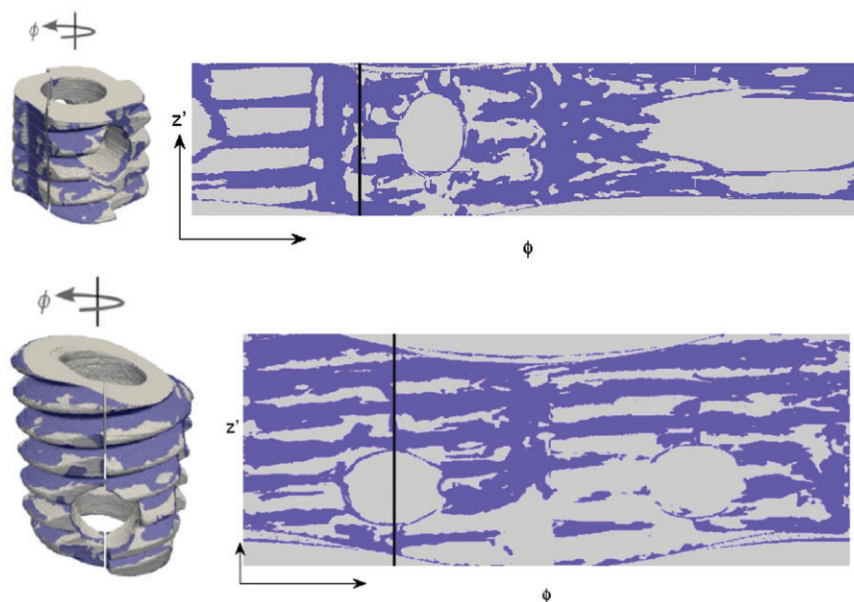


Figure 9 (Left column) Rendered surface of two implants (239 and 240) with bone-implant contact regions superimposed. (Right column) The corresponding unfolded surfaces. Black dashed lines show the approximate location of the peaks of the threads. The vertical line indicates the corresponding angles in the two columns.

bring about major explorative peri-implantitis surgery and the impact of such treatment in terms of resolution is still unclear (for review, see Claffey and colleagues²⁰).

Implant #L3, repaired in 1994 according to the recommendations described by Lekholm and colleagues,²¹ functioned successfully and supported the fixed prosthesis for another 12 years before it was removed in

2006. During the later years, the remaining implants were frequently involved with soft-tissue problems, such as bleeding and pus on probing, and presented a slow but continuous marginal bone resorption. In order to preserve as much bone as possible, all implants, which are still being stable and partly osseointegrated including fragment #R3, were trephined out from the jaw in

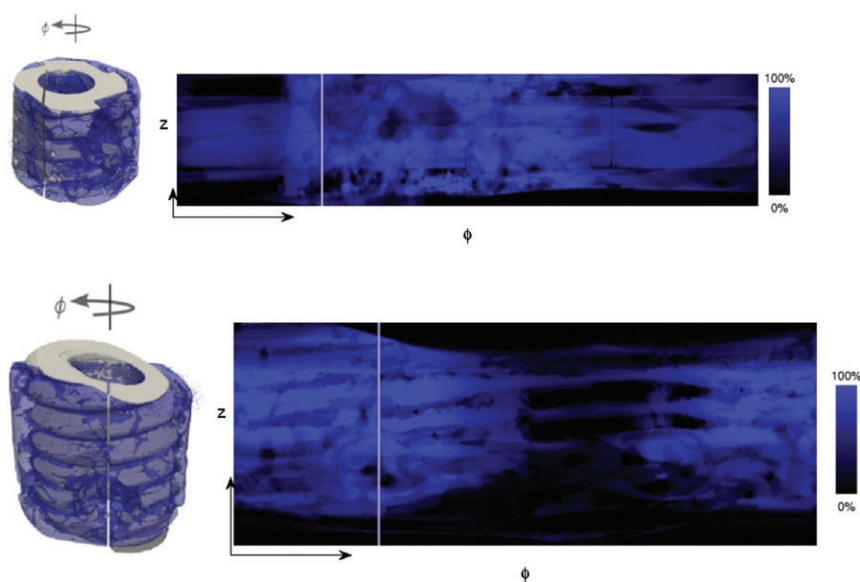


Figure 10 (Left) Rendered surface of two implants (239 and 240) with the bone tissue volume in the region of interest superimposed. (Right) The corresponding unfolded surfaces. White dashed lines show the peaks of the threads. The vertical line indicates the corresponding angles in the two columns.

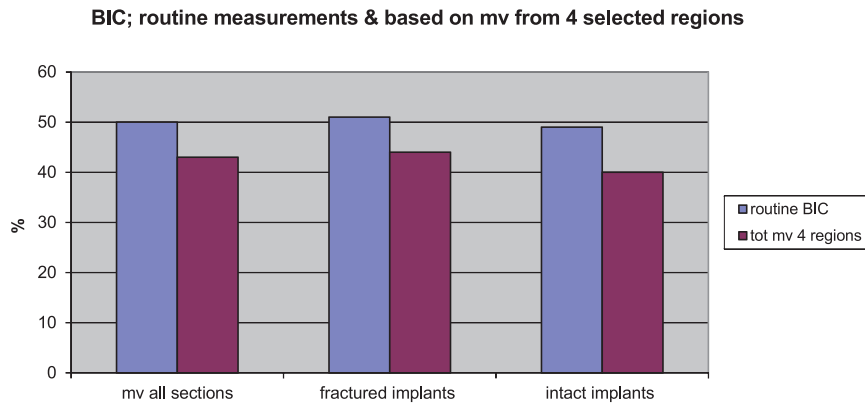


Figure 11 Histomorphometry results based on all five samples and mean values of the three fractured implants and the two intact implants. The mean values of bone-implant contact (BIC) are generated by (i) routine measurements and (ii) based on mean values of four selected regions. The (i) routine measurements are performed from thread-peak to thread-peak while the (ii) “new” measurements of BIC based on four regions along the thread profile take the entire thread geometry into consideration. Approximately 15% lower BIC values are generated with the latter method.

2007. The implants served their purpose and for almost three decades, they provided the patient with a fixed prosthesis. Furthermore, after being removed, the retrieved samples served a second purpose and provided the present authors with valuable information based on utilized laboratory techniques resulting in state-of-the-art and beyond state-of-the-art techniques.

Division of bony contact to show the distribution of BIC in various regions, may roughly reflect the bone-remodeling pattern around the implant.⁴ In the paper by Bolind and colleagues,⁴ the remodeling pattern was observed around nonloaded and implants loaded with various loading times. The unloaded implants had the lowest BIC percentage in the bottom region of the implant and the highest BIC in the apical flank region. With increasing time of loading, the distribution

changed and a loading time of more than 5 years revealed the lowest BIC in the tip region and almost the highest BIC for the bottom region. In the present report, similar observations were found and the lowest BIC percentages were observed in the tip, that is, the implant thread-peak region and highest BIC was found in the bottom region of the tread. The material in the present study is all from maxilla, while the material report by Bolind and colleagues⁴ included a mixture of mandible and maxillary implants, and the exact sites were unknown. The present material was in situ for 29 years and the actual time of loading for each individual implant are not fully known. Nevertheless, this type of BIC quantifications involving selected lengths (including the entire thread peaks) may possibly enhance the understanding of the BRP in relation to implant insertion and loading time. Comparison

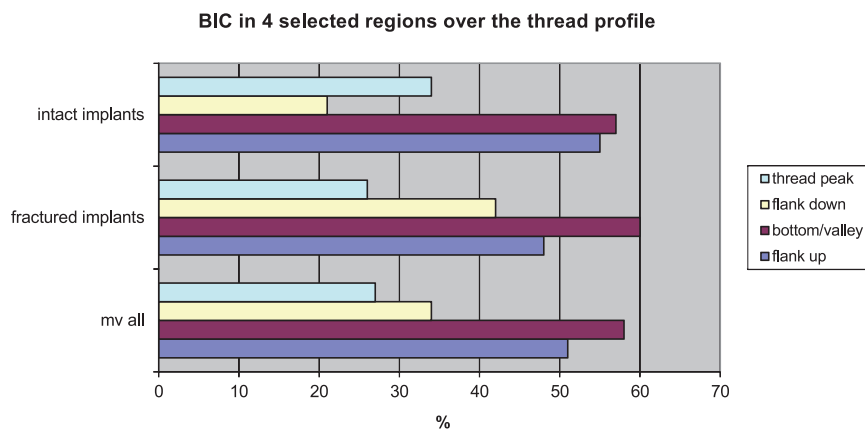


Figure 12 Bone-implant contact (BIC) measured in the four various regions along the thread profile. The bottom region of the thread shows the greatest BIC values while, in general, the lowest BIC was observed in the thread-peak regions.

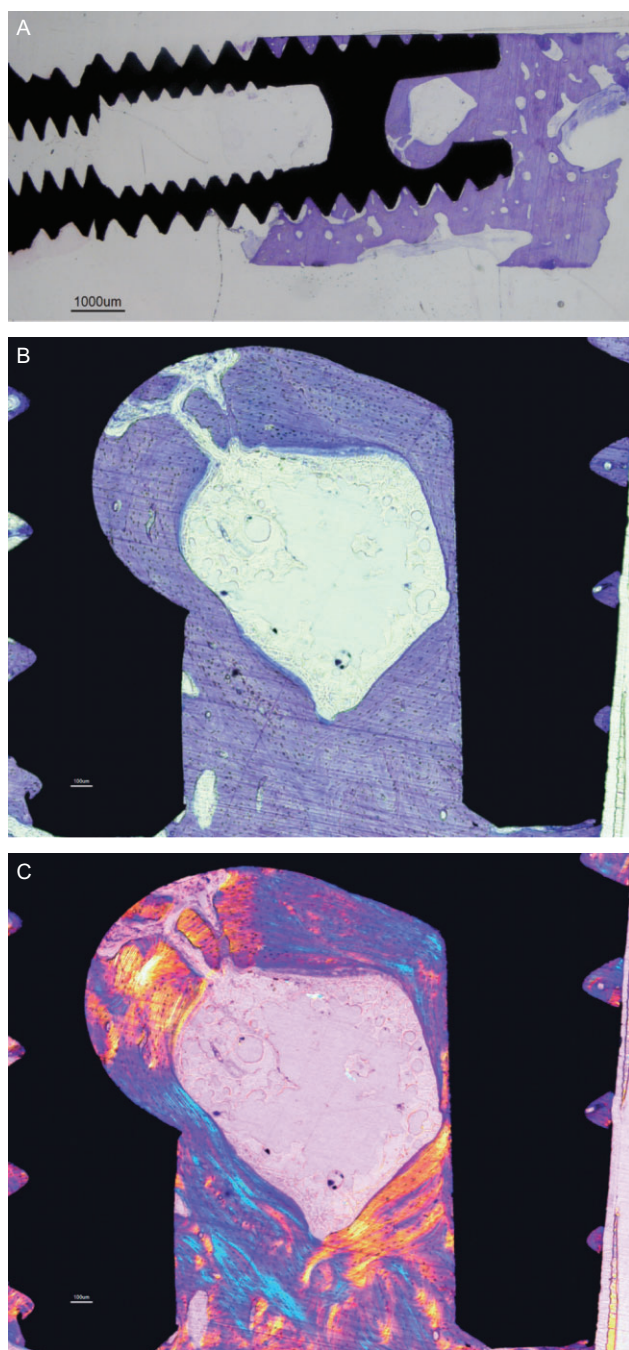


Figure 13 (A) Survey picture of one cut and ground section from of the intact implants with surrounding blue/purple stained (toluidine blue mixed in pyronin G) undecalcified bone. As can be observed, about 50% of the sample is lacking bone tissue. (B) This figure is a close-up of the apical hole region from the intact sample (A) revealing good osseointegration when viewed on the toluidine blue stained undecalcified cut and ground section. (C) The same region as in (B) but visualized with the aid of polarizing filters demonstrating collagen structure in different colors due to the usage of a lambda-filter.

of mean BIC numbers from the two-dimensional and three-dimensional quantification, when presented as an average of the entire surface, revealed 21% less BIC in the two-dimensional quantification. However, Rebaudi and colleagues⁵ presented about 20% greater BIA (bone-implant apposition) obtained with the two-dimensional histomorphometry compared with the μ CT. Reasons for these diverse findings may be that Rebaudi and colleagues⁵ performed two-dimensional measurements on 50- μ m-thick sections compared with the present authors' 15- μ m-thick sections. It is of great importance to work with thin cut and ground sections because thicker sections, that is, more than 30 μ m will result in overestimation of the BIC.¹⁵ Another reason may be due to the differences in "true" comparisons between BIC and BIA. In the present paper, BIC is calculated on cut and ground sections in the bone-implant interface region in the light microscope. BIC calculations, when averaged from the present three-dimensional material, are performed about 11 μ m from the interface. According to Rebaudi and colleagues,⁵ the BIA is defined as "There was bone in a 45- μ m neighborhood of the titanium surface." Moreover, the methods used for analyses vary between the present paper and the one by Rebaudi and colleagues⁵: the former material was imaged by a SR μ CT scanner, whereas the latter used a μ CT scanner to image the samples.

The animations provided information about the osseointegration over the whole sample in an intuitive way. The "two-dimensional unfolding" rendered a direct overview of the BIC of the surface of the implant and the bone concentration in the proximity of the implant.

Thus, the importance of information rendering complete and adequate retrieval protocols are necessary for drawing further conclusions related to the concept of osseointegration of implants. Although being a concept that is regarded as routine today, it seems as we have a lot to learn and, thus, case reports provide valuable information.

CONCLUSION

Applying the novel three-dimensional visualization methods, such as "thread-fly-through" and "two-dimensional unfolding," in relation to traditional two-dimensional histological analysis of osseointegration of oral implants is unique. The novel three-dimensional approaches have the benefit of providing information for the whole sample but cannot substitute the

histological analysis because tissue reactions and biological performances to implants must be observed at the cellular level routinely. The latter statement counts for what we know today, but we are already gaining knowledge related to other resolution levels like proteins and genes and their involvement in the fascinating concept of osseointegration.

As adequate three-dimensional imaging of implants requires large-scale imaging facilities, the three-dimensional methods cannot be applied routinely but as the desktop three-dimensional imaging techniques evolve, tomorrow's researchers are to benefit from such methods.

ACKNOWLEDGMENTS

Professor Per-Ingvar Brånemark and Dr. Ragnar Adell performed the surgery together and are acknowledged for being an inspiration to the entire world of osseointegration. The implants were retrieved at the Brånemark Clinic in Göteborg. The samples were processed at SR μ CT within the grant IA-SFS project RII3-CT-2004-506008. Sections were prepared by Ms. Petra Johansson and Ms. Ann Albrektsson at the laboratories of Biomaterial Sciences, Göteborg University. Else Huijbers is greatly acknowledged for her comments on the linguistics of the manuscript. This work was supported by grants from The Knowledge Foundation, project 2008/0716.

REFERENCES

1. Shibli JA, Aguiar KCDS, Melo L, d'Avila S, et al. Histological comparison between implants retrieved from patients with and without osteoporosis. *Int J Oral Maxillofac Surg* 2008; 37:321–327.
2. Uehara T, Takaoka K, Ito K. Histological evidence of osseointegration in human retrieved fractured hydroxyapatite-coated screw-type implants: a case report. *Clin Oral Implants Res* 2004; 15:540–545.
3. Danilo DS, Iezzi G, Scarano A, Perrotti V, Piattelli A. Immediately loaded blade implant retrieved from a man after 20-year loading period: a histologic and histomorphometric case report. *J Oral Implantol* 2006; 32:171–176.
4. Bolind P, Johansson CB, Balshi TJ, Langer B, Albrektsson T. A study of 275 retrieved Brånemark oral implants. *Int J Periodontics Restorative Dent* 2005; 05:425–437.
5. Rebaudi A, Koller B, Laib A, Trisi P. Microcomputed tomographic analysis of the peri-implant bone. *Int J Periodontics Restorative Dent* 2004; 24:316–325.
6. Stoppie N, van der Waerden J-P, Jansen JA, Duyck J, Wevers M, Naert IE. Validation of microfocus computed tomography in the evaluation of bone implant specimens. *Clin Implant Dent Relat Res* 2005; 7:87–94.
7. Butz F, Ogawa T, Chang T-L, Nishimura I. Three-dimensional bone-implant integration profiling using micro-computed tomography. *Int J Oral Maxillofac Implants* 2006; 21:687–695.
8. Ko C-Y, Lim D, Choi B-H, Li J, Kim H-S. Suggestion of new methodology for evaluation of osseointegration between implant and bone based on μ -CT images. *Int J Precision Eng Manuf* 2010; 11:785–790.
9. Bernhardt R, Scharnweber D, Müller B, et al. Comparison of microfocus- and synchrotron X-ray tomography for the analysis of osseointegration around Ti6AL4V-implants. *Eur Cell Mater* 2004; 7:42–50.
10. Weiss P, Le Nihouannen D, Rau C, et al. Synchrotron and non synchrotron X-ray microtomography threedimensional representation of bone ingrowth in calcium phosphate biomaterials. *Eur Cell Mater* 2005; 9:48–49.
11. Lindhe J, Meyle J. Peri-implant diseases: consensus report of the sixth European workshop on periodontology. *J Clin Periodontol* 2008; 35:282–285.
12. Donath K, Breuner G. A method for the study of undecalcified bones and teeth with attached soft tissues. *J Oral Pathol* 1982; 11:318–326.
13. Johansson CB, Morberg P. The importance of ground section thickness for reliable histomorphometrical results. *Biomaterials* 1995; 16:91–95.
14. Johansson CB, Albrektsson T. A removal torque and a histomorphometric study of commercially pure niobium and titanium implants in rabbit bone. *Clin Oral Implants Res* 1991; 2:24–29.
15. Barrett J, Keat N. Artifacts in CT: recognition and avoidance. *Radiographics* 2004; 24:1679–1691.
16. Sarve H, Lindblad J, Johansson CB. Quantification of bone remodeling in SR μ CT images of implants. *Lecture Notes Computer Sci* 2009; 5575:770–779.
17. Cancedda R, Cedola A, Giuliani A, et al. Bulk and interface investigations of scaffolds and tissue engineered bones by X-ray microtomography and X-ray microdiffraction. *Biomaterials* 2007; 28:2506–2521.
18. Sarve H, Lindblad J, Borgefors G, Johansson CB. Methods for visualization of bone tissue in the proximity of implants. *Lecture Notes Computer Sci* 2010; 6375:243–250.
19. Sarve H, Lindblad J, Borgefors G, Johansson CB. Extracting 3D information on bone remodeling in the proximity of titanium implants in SR μ CT image volumes. *Comput Methods Programs Biomed* 2011; 102:25–34.
20. Claffey N, Clarke E, Polyzois I, Renvert S. Surgical treatment of peri-implantitis. *J Clin Periodontol* 2008; 35:316–332.
21. Lekholm U, Adell R, Brånemark P-I. Possible complications. In: Brånemark P-I, Zarb G, Albrektsson T, eds. *Tissue integrated prostheses – osseointegration in clinical dentistry*. Chicago, IL: Quintessence Publ Co, 1985:233–240.

Copyright of Clinical Implant Dentistry & Related Research is the property of Wiley-Blackwell and its content may not be copied or emailed to multiple sites or posted to a listserv without the copyright holder's express written permission. However, users may print, download, or email articles for individual use.